Supporting Information

Tailoring the cellulose paper via electroless CuSnB deposition for the selective electrochemical detection of dopamine

Alankar Kafle, Divyani Gupta, Daisy Mehta and Tharamani C. Nagaiah*

Department of Chemistry, Indian Institute of Technology Ropar, Rupnagar, Punjab-140001, India

Email: tharamani@iitrpr.ac.in

Experimental

Materials

Stannous chloride (SnCl$_2$), copper sulphate (CuSO$_4$.5H$_2$O), trisodium citrate (Na$_3$C$_6$H$_5$O$_7$), were bought from Loba chemie. Ethanol (C$_2$H$_5$OH, 99.9%), and acetone (CH$_3$COCH$_3$, 99%) were purchased from Rankem. Similarly, Dopamine hydrochloride (>99% crystalline), ascorbic acid (99% crystalline), uric acid, KH$_2$PO$_4$ and K$_2$HPO$_4$ were bought from Sigma-Aldrich whereas dopamine hydrochloride injections (40 mg mL^{-1}) was purchased from Neon Laboratories Ltd. Deionized water obtained from Millipore system (>15 MΩ) was employed for the preparation of solutions and all the chemicals were used as received without any further purification.

Fabrication of paper electrodes

Fabrication of VC-CP: Whatman filter paper of size 1cm × 1cm was dipped in acetone and sonicated for five minutes then thoroughly washed with deionised water and dried in hot air oven at 60 °C. The dried cellulose paper was coated with the Vulcan carbon paste (Vulcan carbon: PVDF, 3:1) dispersed in NMP and dried at 60 °C for complete dryness.

Fabrication of CuSnB/VC-CP:

The carbon coated cellulose paper (VC-CP) was dipped in 15 mL ice cold solution containing 3.75 mmole SnCl$_2$, 1.25 mmole CuSO$_4$ and 2.5 mmole trisodium citrate and further kept in an ice bath in which sodium borohydride solution (12 mmole NaBH$_4$ in 10 mL deionized water) was slowly added from the walls of the container and kept as such till the effervescence siezed. After the completion of the reaction the paper substrate was washed thoroughly with deionized water and finally with ethanol water (1:1) solution and dried at 60 °C in hot air oven. Similarly, fabrication of control electrodes i.e. CuB/VC-CP and SnB/VC-CP were performed by taking

respective metal salt only with the same procedure. The copper and tin ratio was optimized by varying the molar ratio of Cu and Sn from 1:1, 1:2, 1:3, 2:1 and 3:1 by keeping the total no. of moles of metal salt to be similar.

Physical characterization

The structural investigation of the prepared electrode was studied with powder X-ray diffraction by using PANalytical X'PERT pro diffractometer containing Cu-Kα radiation (λ=0.1542 nm, 40kV, 40mA) within the 2θ range of 5-80° at a scan rate of 5° per minute and a proportional counter detector. The scanning electron microscopy (SEM, JEOL, JSM-6610LV) and field emission-scanning electron microscopy (FE-SEM, Hitachi, Japan, SU8010) were employed to study the morphology of the materials. The elemental surface composition of the material was analysed by X-ray photoelectron spectroscopy (XPS) which was performed by using Thermo scientific NEXSA surface analysis containing a micro-focused (400 μm, 72 W, 12000 V) monochromatic Al Kα (1486.6 eV), a hemispherical analyser and 128 channel plate detectors under ultrahigh vacuum (UHV 8-10 mbar). The obtained spectra was calibrated with respect to C 1s spectra.

Electrochemical measurements

In order to perform the electrochemical investigations Biologic (VSP 300) potentiostat/ galvanostat with an FRA7M module, controlled by EC-Lab V11.12 software was employed in a three-electrode set up where as fabricated CuSnB/VC-CP used as working electrode (WE) whereas, Pt wire and Ag/AgCl/3 M KCl were used as counter electrode (CE) and reference electrode (RE) respectively. Similarly, 0.1 M phosphate buffer solution (pH 7.0) was used as electrolyte. The electrochemical impedance spectroscopy (EIS) was employed to measure the charge transfer resistance which were conducted at a DC voltage of 190 mV over a frequency range between 5 Hz to 2.0 MHz.
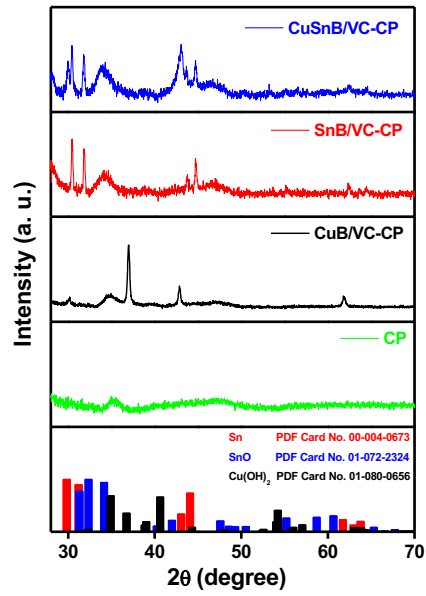
Fig. S1. Comparison of the PXRD pattern for bare cellulose paper, CuB/VC-CP, SnB/VC-CP and CuSnB/VC-CP electrodes.
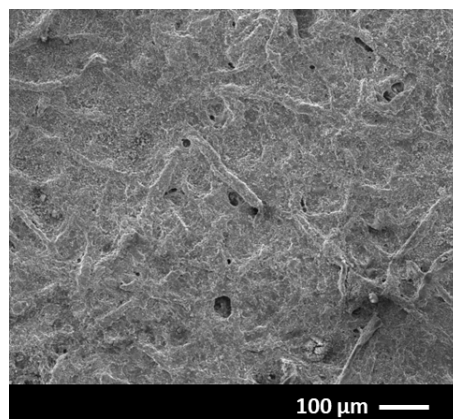

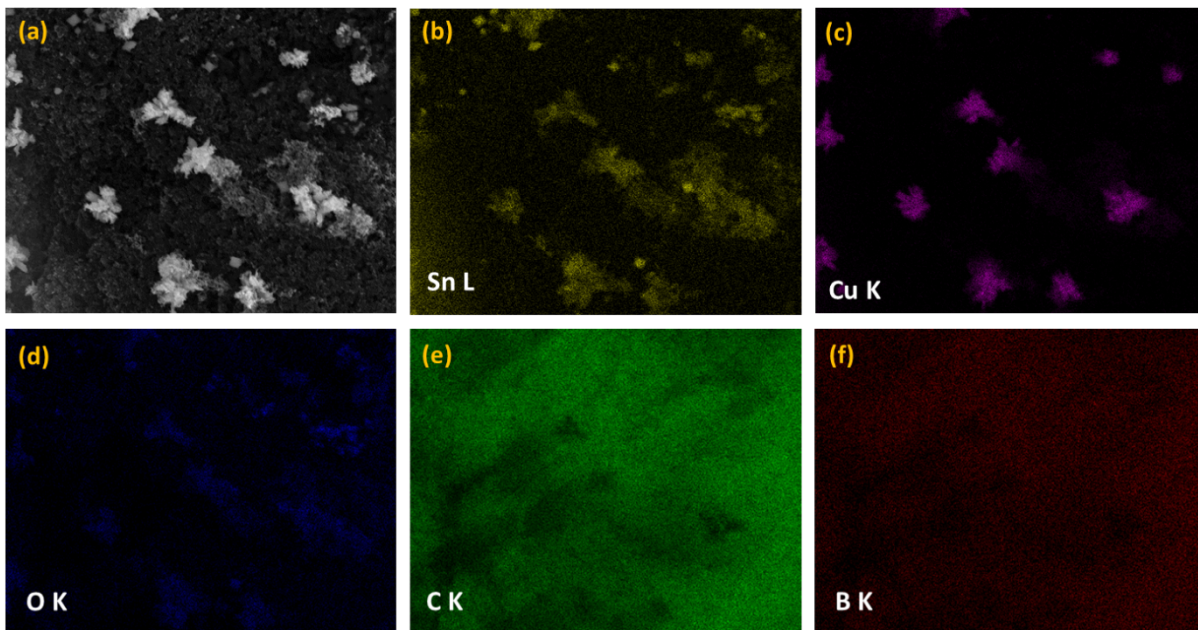**Fig. S2.** SEM image of Vulcan Carbon (VC) coated cellulose paper.

Fig. S3. (a) FE-SEM image of selected area and corresponding elemental dot mapping images of elements, (b) Sn, (c) Cu, (d) O (e) C and (f) B for SnCuB/VC-CP electrode.
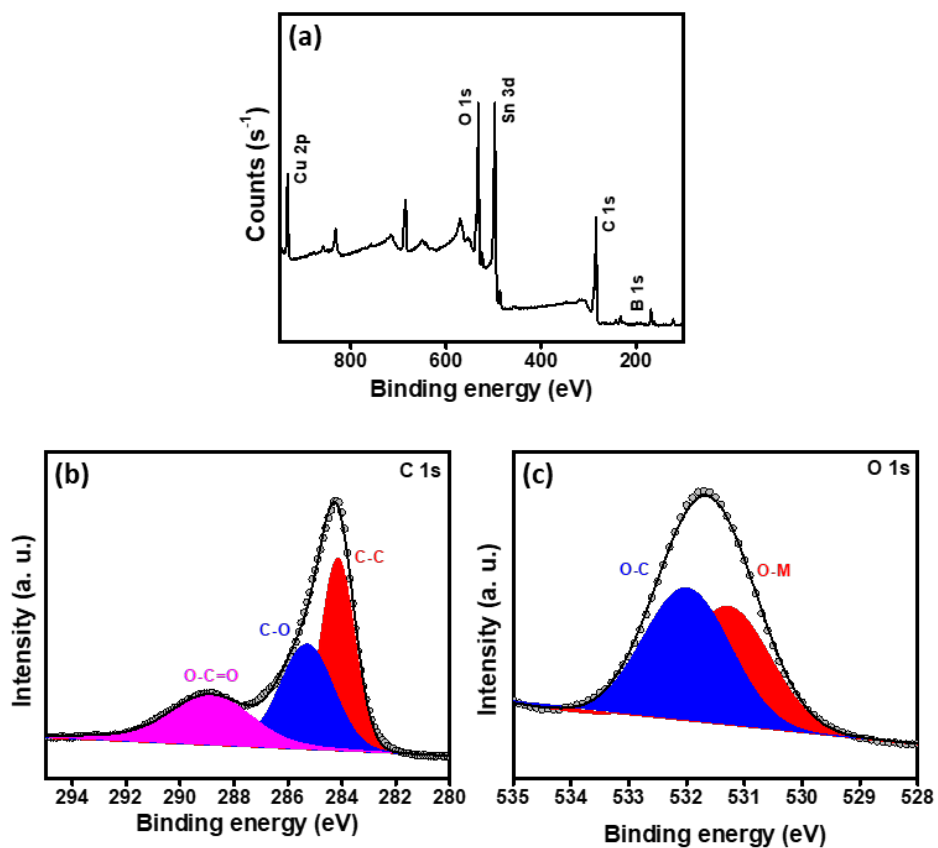

Fig. S4A. (a) XPS survey spectra and deconvoluted XP spectra of (b) C 1s and, (c) O 1s for CuSnB/VC-CP.
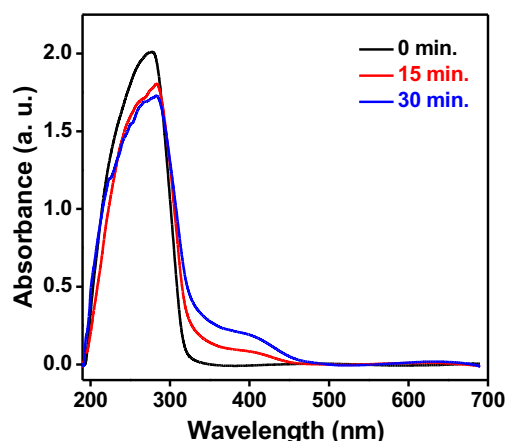
Fig. S4B. *In situ* UV spectra recorded during the chronoamperometric measurement of CuSnB/VC-CP in 0.1M PBS (pH 7.0) electrolyte containing 200 µM DA and 200 µM AA.

The reduction of absorbance at $\lambda = 280$ nm (corresponding to DA) with time evolution indicated the decreasing of dopamine concentration whereas appearance of new peak at $\lambda = 395$ nm (corresponding to the dopamine-o-quinone) at the same time evidenced the formation of dopamine-o-quinone as an oxidation product.[1] On the basis of this evidence, it is confirmed that the peak observed at 0.2 V vs. Ag/AgCl (3M KCl) is due to the oxidation of dopamine and the oxidation product is dopaminoquinone.

Electrochemical impedance spectroscopy (EIS)

The electrochemical impedance spectroscopy (EIS) was employed to measure the charge transfer resistance which were conducted at a DC voltage of 190 mV over a frequency range between 5 Hz to 2.0 MHz.

The enhanced activity of CuSnB/VC-CP towards the electrooxidation of dopamine is related to the interfacial charge transfer kinetics which can be explained with the help of Nyquist plot. The charge transfer resistance (Rct) is directly related to the kinetics of the electrode reaction as the higher Rct indicates the slower kinetics whereas lower value specifies the facile kinetics

towards electrode reaction. The lowest charge transfer resistance of CuSnB/VC-CP in comparison to monometallic variant (Fig. 3a) evidenced the enhanced charge transfer kinetics in the electrode electrolyte interface. The enhanced activity of bimetallic variant CuSnB/VC-CP could be due to the modification in electronic structure of the material after the addition of second metal which could result the synergistic effect.[2]

Electrochemical surface area (ECSA):

The electrochemical surface area of the electrodes was calculated with the help of double-layer pseudo-capacitance (C_{dl}). For this, a series of cyclic voltammetry measurements were performed in the non-faradic potential region of -0.1 V to 0.1 V *vs.* RHE with various scan rate from 40 to 140 mV s^{-1}. The C_{dl} was obtained as a slope from the graph of average current density ($j_c + j_a$) versus the scan rate. Thereafter, the ECSA was determined by dividing the C_{dl} by the average specific capacitance of the flat standard surface 40 μF cm^{-2}.

The ECSA is another key parameter for the determination of the kinetics of the electrode reaction. Higher the value of ECSA, greater is the number of electrochemical active sites and consequently the electrode reaction kinetics is more facile. The combination of two individual metals causes the modification in electronic structure of the material as a result the increment in the number of active sites will occur and moreover, larger ECSA of bimetallic variant than respective monometallic variant signifies that the synergistic effect is responsible for the higher no. of exposed sites due to the combination of two individual metals.[3] The CuSnB/VC-CP electrode demonstrated the higher ECSA than their monometallic variant electrodes which further supported the improved kinetics of the CuSnB/VC-CP electrode over CuB/VC-CP and SnB/VC-CP electrodes. (Fig. S5 and Table S1).
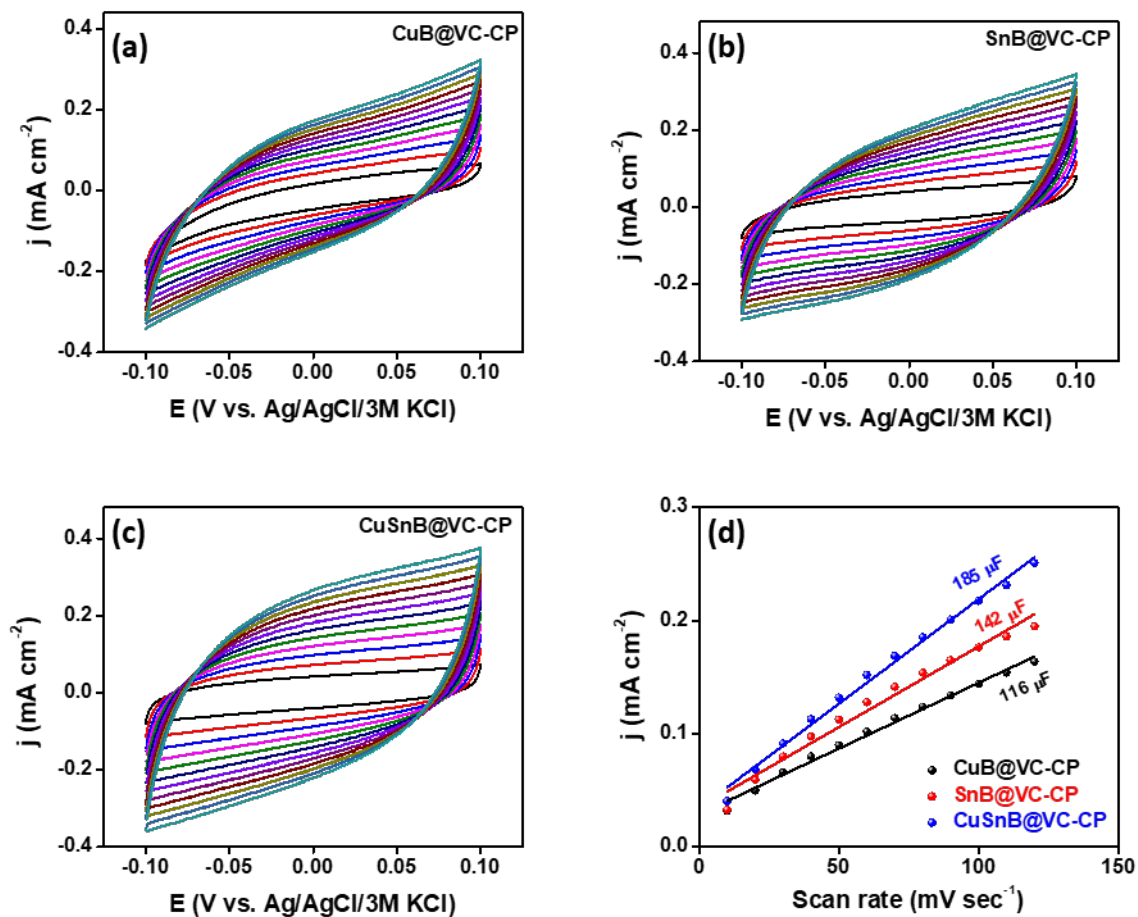
Fig. S5. Cyclic voltammograms of (a) CuB/VC-CP and (b) SnB/VC-CP and (c) CuSnB/VC-CP in non-faradic potential region at various scan rates and (d) corresponding average current density versus scan rate plot for ECSA determination.

Table S1: Electrochemical surface area (ECSA) determination.

S. No.	Composite	C_{dl} (μF)@ 0.0 V *vs.* Ag/AgCl/3M KCl	ECSA (cm^2)
1	CuB/VC-CP	116	2.9
2	SnB/VC-CP	142	3.55
3	CuSnB/VC-CP	185	4.63
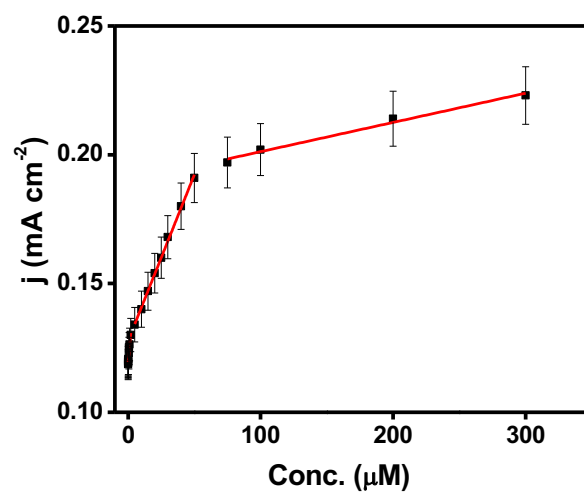
Fig. S6. Plot of current density versus concentration of DA for CuSnB/VC-CP electrode extracted from Fig. 2g.
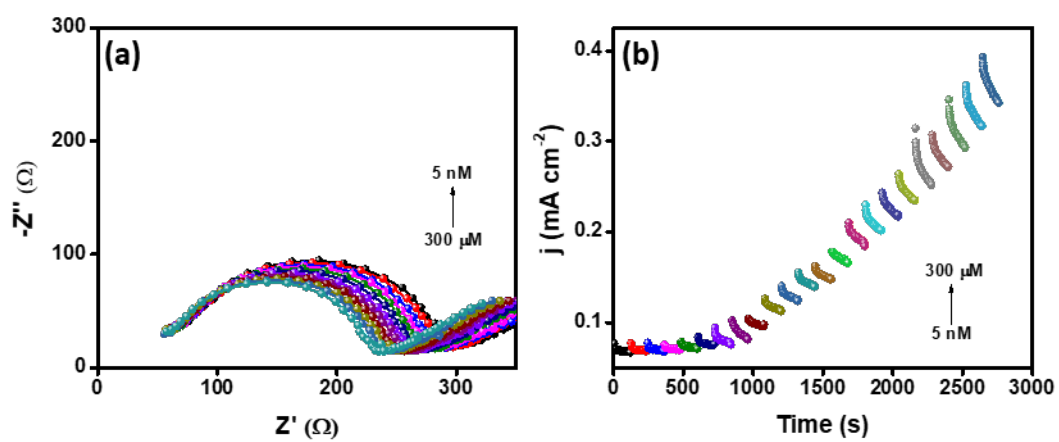

Fig. S7. (a) EIS and (b) chronoamperometric response of flexible CuSnB/VC-CP electrodes in 0.1 M PBS electrolyte containing 200 mM AA and various concentrations of DA.
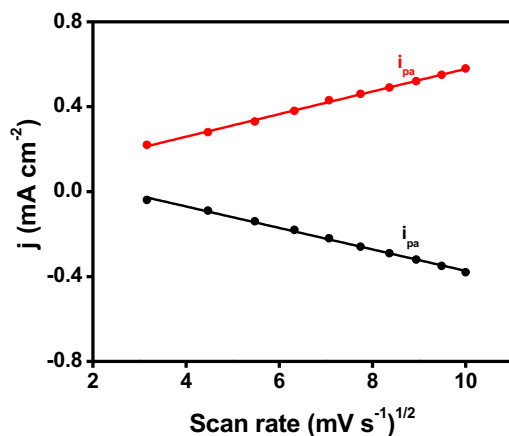
Fig. S8. Peak current density versus square root of scan rate curve extracted from Fig. 2h.
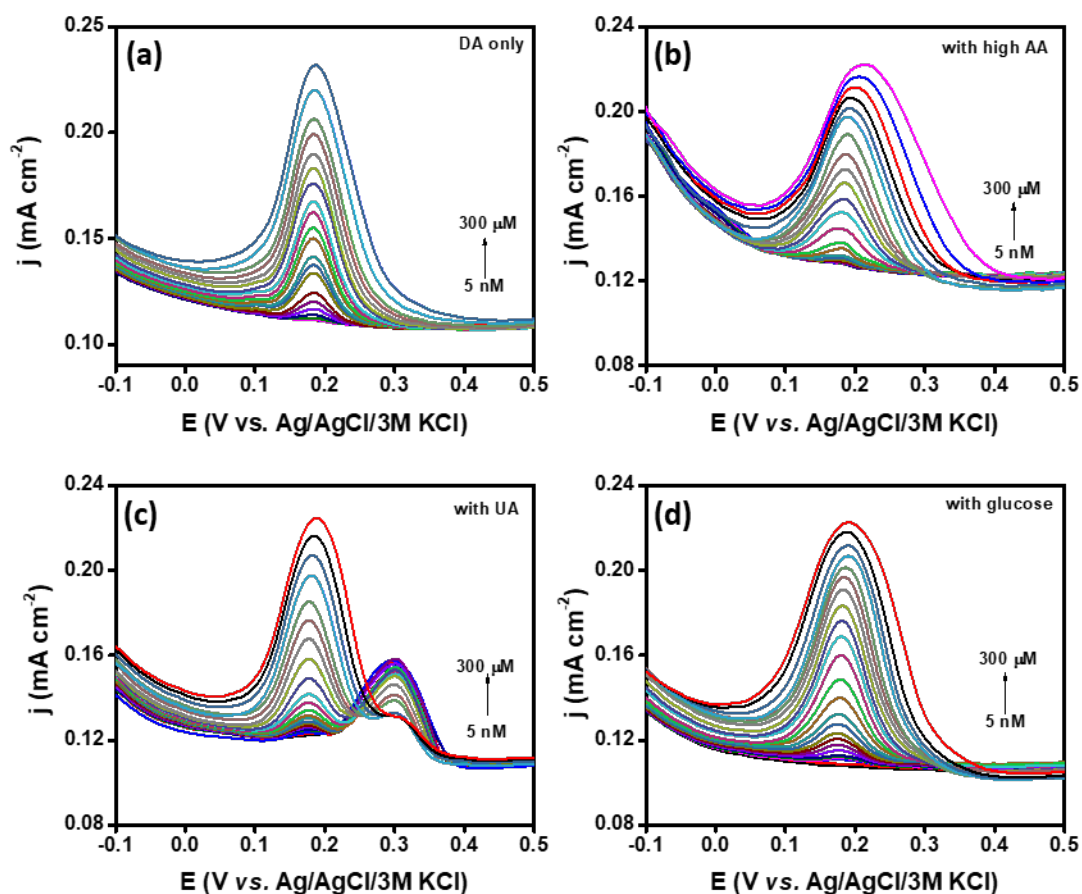

Fig. S9. Differential pulse voltammogram of CuSnB/VC-CP (a) in the absence of interferents and in presence of interferants (b) 1000 μM AA, (c) 200 μM UA and (d) 3000 μM glucose at various concentrations of DA with step height of 10 mV and pulses width of 900 ms.
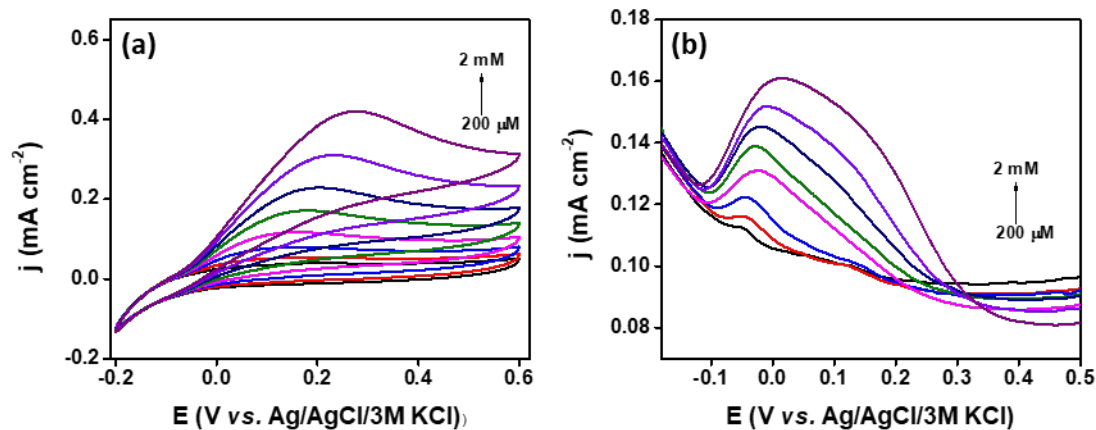
Fig. S10. (a) CV and (b) DPV of CuSnB/VC-CP in 0.1 M PBS (pH 7.0) electrolyte containing various concentrations of AA (DPV: step height 10 mV and pulses width 900 ms).

Fig. S11. (a) CV and (b) DPV of CuSnB/VC-CP in 0.1 M PBS (pH 7.0) electrolyte containing various concentrations of UA (DPV: step height 10 mV and pulses width 900 ms).
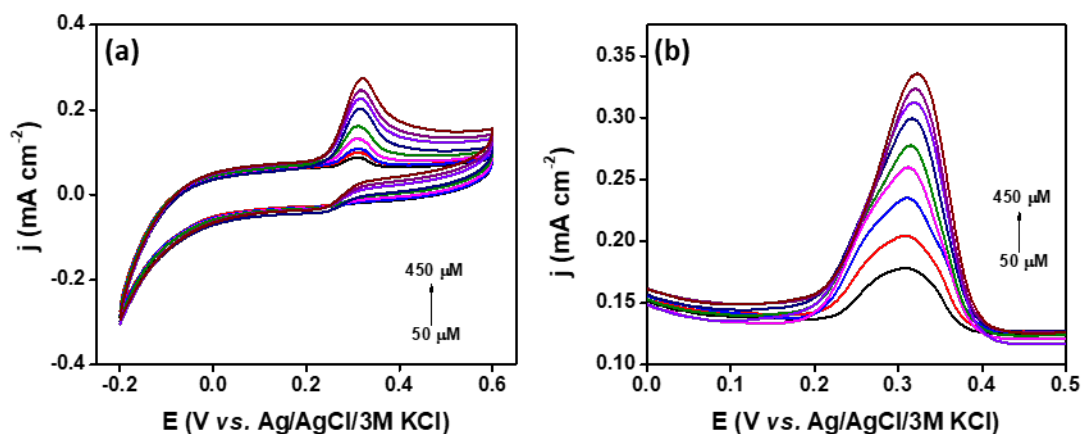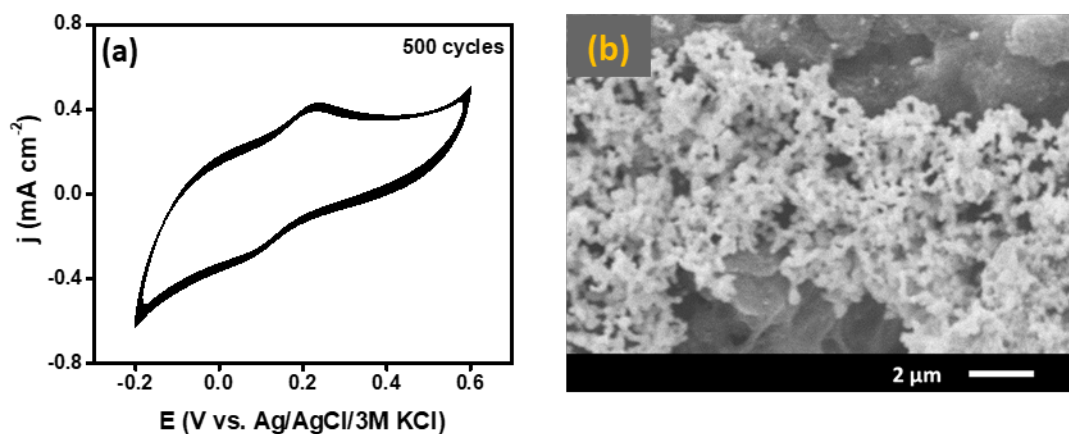
Fig. S12. (a) Cyclic voltammograms of CuSnB/VC-CP in 0.1M PBS (pH 7.0) electrolyte containing 200 μM DA and 200 μM AA for 100 cycles at a scan rate of 50 mV s^{-1} (b) SEM image of CuSnB/VC-CP catalyst after 100 CV cycling in 0.1 M PBS electrolyte containing 200 μM DA and 200 μM AA at a scan rate of 50 mVs^{-1}.
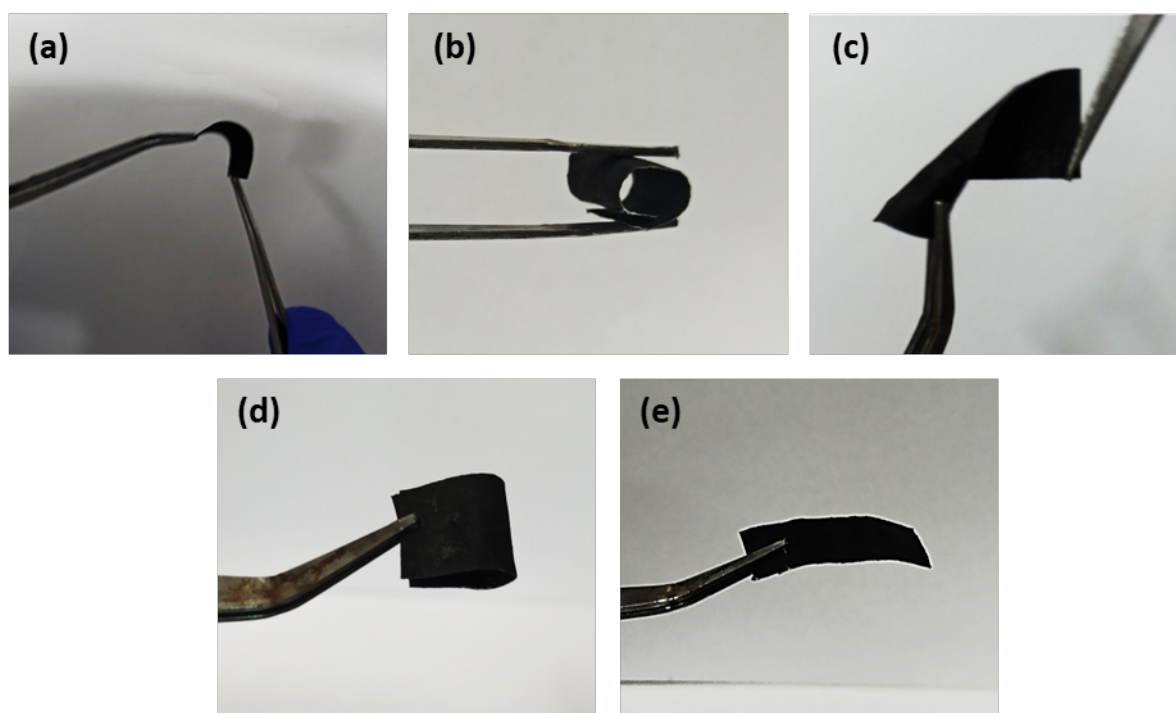

Fig. S13. Photographs of the electroless deposited flexible paper electrode under (a) bending, (b) rolling, (c) twisting, (d) folding and (e) relaxing conditions.

Table S2. Analytical results of CuSnB/VC-CP electrode towards determination of dopamine from commercially available dopamine hydrochloride injection.

S. No.	Conc. (taken)	Conc. (added)	Conc. (actual)	Conc. (found)	Recovery (%)
1	5 µM	5 µM	10 µM	10.1	101
2	5 µM	10 µM	15 µM	14.6	97
3	5 µM	20 µM	25 µM	26	104

Table S3. Analytical results of CuSnB/VC-CP electrode towards determination of dopamine in urine sample.

S. No.	Conc. (added)	Conc. (found)	Recovery (%)
1	10 µM	9.96	99.6
2	20 µM	20.95	104
3	30 µM	29.22	97.4
4	40 µM	37.96	95

References

1. M. Bisaglia, S. Mammi and L. Bubacco, *J. Biol. Chem.*, 2007, **282**, 15597-15605.
2. N. Thakur, A. Chaturvedi, D. Mandal and T. C. Nagaiah, *Chem. Commun.*, 2020, **56**, 8448-8451.
3. H. Huang, A. Cho, S. Kim, H. Jun, A. Lee, J. W. Han and J. Lee, *Adv. Funct. Mater.*, 2020, **30**, 2003889.